

©2005 IEEE. Personal use of this material is permitted. However, permission to reprint/republish this material for advertising or promotional purposes or for creating new collective works for resale or redistribution to servers or lists, or to reuse any copyrighted component of this work in other works must be obtained from the IEEE.

Report Documentation Page				Form Approved OMB No. 0704-0188	
Public reporting burden for the collection of information is estimated to average 1 hour per response, including the time for reviewing instructions, searching existing data sources, gathering and maintaining the data needed, and completing and reviewing the collection of information. Send comments regarding this burden estimate or any other aspect of this collection of information, including suggestions for reducing this burden, to Washington Headquarters Services, Directorate for Information Operations and Reports, 1215 Jefferson Davis Highway, Suite 1204, Arlington VA 22202-4302. Respondents should be aware that notwithstanding any other provision of law, no person shall be subject to a penalty for failing to comply with a collection of information if it does not display a currently valid OMB control number.					
1. REPORT DATE OCT 2004		2. REPORT TYPE		3. DATES COVERED 00-00-2004 to 00-00-2004	
4. TITLE AND SUBTITLE Fabrication Development for Nanowire GHz-Counting-Rate Single-Photon Detectors				5a. CONTRACT NUMBER	
				5b. GRANT NUMBER	
				5c. PROGRAM ELEMENT NUMBER	
6. AUTHOR(S)				5d. PROJECT NUMBER	
				5e. TASK NUMBER	
				5f. WORK UNIT NUMBER	
7. PERFORMING ORGANIZATION NAME(S) AND ADDRESS(ES) Massachusetts Institute of Technology,Cambridge,MA,02139				8. PERFORMING ORGANIZATION REPORT NUMBER	
9. SPONSORING/MONITORING AGENCY NAME(S) AND ADDRESS(ES)				10. SPONSOR/MONITOR'S ACRONYM(S)	
				11. SPONSOR/MONITOR'S REPORT NUMBER(S)	
12. DISTRIBUTION/AVAILABILITY STATEMENT Approved for public release; distribution unlimited					
13. SUPPLEMENTARY NOTES					
14. ABSTRACT We have developed a fabrication process for GHz-counting-rate, single-photon, high-detection-efficiency NbN, nanowire detectors. We have demonstrated two processes for the device patterning, one based on the standard polymethylmethacrylate (PMMA) organic positive-tone electron-beam resist and the other based on the newer hydrogen silsesquioxane (HSQ) negative-tone spin-on-glass resist. The HSQ-based process is simple and robust, providing high resolution and the prospect of high fill-factors. Initial testing results show superconductivity in the films, and suggest that the devices exhibit photosensitivity.					
15. SUBJECT TERMS					
16. SECURITY CLASSIFICATION OF:			17. LIMITATION OF ABSTRACT Same as Report (SAR)	18. NUMBER OF PAGES 6	19a. NAME OF RESPONSIBLE PERSON
a. REPORT unclassified	b. ABSTRACT unclassified	c. THIS PAGE unclassified			

Fabrication Development for Nanowire GHz-Counting-Rate Single-Photon Detectors

Joel K. W. Yang, Eric Dauler, Antonin Ferri, Aaron Pearlman, Aleksandr Verevkin, Gregory Gol'tsman, Boris Voronov, Roman Sobolewski, William E. Keicher, and Karl K. Berggren

Abstract—We have developed a fabrication process for GHz-counting-rate, single-photon, high-detection-efficiency, NbN, nanowire detectors. We have demonstrated two processes for the device patterning, one based on the standard polymethylmethacrylate (PMMA) organic positive-tone electron-beam resist, and the other based on the newer hydrogen silsesquioxane (HSQ) negative-tone spin-on-glass resist. The HSQ-based process is simple and robust, providing high resolution and the prospect of high fill-factors. Initial testing results show superconductivity in the films, and suggest that the devices exhibit photosensitivity.

Index Terms—Epitaxial niobium-nitride thin films, hydrogen silsesquioxane electron-beam resist, superconductive single-photon detectors.

I. INTRODUCTION

WE HAVE developed two fabrication processes to produce structures for superconductive GHz-counting-rate single-photon detectors [1]–[5]. Both of these processes were based on electron-beam lithography processes, one with PMMA and the other with HSQ, and were used to pattern nanowire meander structures in a ~ 4 -nm-thick epitaxial NbN film [6]. With the PMMA process, we fabricated 225-nm-wide nanowire photodetector structures with a 75% fill factor over an area of $15\ \mu\text{m} \times 15\ \mu\text{m}$. Using the HSQ process, we fabricated 90 nm wide nanowire meander structures with a 50% fill factor over an area of $8\ \mu\text{m} \times 6\ \mu\text{m}$ and demonstrated superconductive single wires as narrow as 50 nm. To achieve uniform linewidth across the detector, an electron beam proximity effect correction technique has been developed. We also investigated the effectiveness of HSQ and PMMA as protective masks when etching NbN. Finally we report initial DC test results of fabricated structures meant to measure NbN sheet resistance and evaluate the superconductivity of nanowires. Tests indicate photosensitivity in the nanowires.

Manuscript received October 4, 2004. This work was sponsored by the United States Air Force under Air Force Contract #F19628-00-C-0002.

J. K. W. Yang and K. K. Berggren are with the Massachusetts Institute of Technology, Cambridge, MA 02139 USA (e-mail: berggren@mit.edu).

E. Dauler and W. E. Keicher are with the Massachusetts Institute of Technology Lincoln Laboratory, Lexington, MA 02420 USA.

A. Ferri was with the Massachusetts Institute of Technology, Cambridge, MA 02139 USA. He is now with Ecole Normale Supérieure, Paris, France.

A. Pearlman and A. Verevkin are with the University of Rochester, Rochester, NY 14627 USA.

G. Gol'tsman and B. Voronov are with Moscow State Pedagogical University, Moscow, Russia.

R. Sobolewski is with the University of Rochester, Rochester, NY 14627 USA, and is also with the Institute of Physics, Polish Academy of Sciences, PL-02668 Warszawa, Poland.

Digital Object Identifier 10.1109/TASC.2005.849971

There are urgent technological needs for GHz-counting-rate photodetectors sensitive to single photons in the infrared region of the spectrum. There are three main applications for this technology: (1) increasing the bandwidth of ultra-low-receive-power free-space optical communication systems so that they might be used for high-bandwidth interplanetary communications; (2) testing high-speed semiconductor circuits, whose failure can be detected and localized by the emission of low levels of infrared light from the damaged circuit regions; and (3) increasing the security of optical communications through the use of single-photon-based quantum communication methods. We are currently developing nanometer-length-scale superconductive photodetectors that will have detection efficiencies and speeds sufficient to meet the demands of these applications. These detectors have performance specifications that exceed by several orders of magnitude those of competing semiconductor-based devices operating in the infrared region of the spectrum.

In this paper, we present details of the fabrication processes that we have developed and discuss the problems that were encountered in this development. Then we describe the test structures that we used and our measurement results. Finally, we describe plans for our future efforts.

II. FABRICATION

A. Device-Level Constraints on Fabrication

The physics of operation for nanowire detectors is based on the formation of a resistive barrier upon absorption of a single photon with sufficient energy [7]. As a photon is absorbed somewhere along a superconducting nanowire that has been biased close to its critical current, a local hotspot is formed that forces the supercurrent to flow around it. If the wire is narrow enough (100 nm or less), the critical-current-density is exceeded in the regions adjacent to the hot spot and phase slip centers will appear across the wire, leading to a measurable voltage pulse that lasts for ~ 70 ps. This mechanism for photodetection leads to two fabrication requirements that have to be met in order to attain high detection efficiencies: (1) narrow wires; and (2) uniform wire linewidth.

Practical considerations associated with the device application also come into play in developing the fabrication process: the devices need to have large areas, to reduce demands on the focusing and alignment precision of the optical path; and the devices need to absorb as many of the incident photons as possible. These considerations result in the need to develop large detector areas and high fill-factors, respectively.

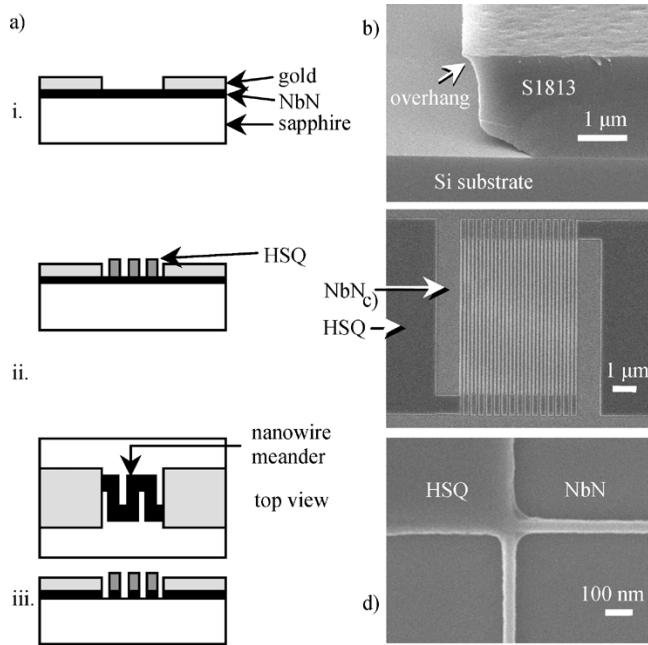


Fig. 1. (a) Flow for a simple three-step process for patterning nanowires. Process details are provided in the text. (a.i) Gold contact pads were electron beam evaporated onto NbN-coated samples and defined through a liftoff process. (a.ii) The pattern was then written in negative electron beam resist, HSQ, and developed. Writes were done using electron-beam lithography. (a.iii) The pattern was then transferred into NbN using RIE. (b) SEM of an overhang structure which facilitates the liftoff process formed by using a post-exposure chlorobenzene dip prior to resist development. (c) SEM of a nanowire pattern with a linewidth of 90 nm and a fill-factor of 50% achieved using the process described in (a). (d) SEM of a test pattern consisting of two perpendicular 50 nm wide nanowires connected to a larger pad defined in HSQ.

Fabricating a photodetector within the constraints outlined above requires the use of high-resolution electron-beam lithography to define narrow and uniform wires in resist. The pattern can then be transferred into the epitaxial niobium nitride (NbN) thin film by using reactive-ion etching (RIE). We have developed two different processes based on this overall outline, which we will describe in turn.

B. Description of HSQ-Based Process

We have developed a simple new process using HSQ electron-beam resist. It required only a single step each of contact photolithography, aligned electron-beam lithography, and etching. This process outline is described in Fig. 1(a). The following are the process details for this method.

- 1) *Liftoff*. In this step, gold contact pads were deposited by electron beam evaporation onto the NbN-coated samples. Windows where the gold would ultimately be deposited were first formed in Shipley Microposit S1813 photoresist by using contact photolithography. Because a highly collimated beam of gold atoms was used for the gold pad deposition, typically a vertical resist sidewall profile would be adequate for lithography. However, because we worked on very small samples where the deposited resist film had highly nonuniform thickness, a

large gap between the substrate and the mask was unavoidable resulting in poor image contrast and sloped resist sidewalls. To assist the liftoff process given this constraint an undercut profile in the photoresist was used as shown in Fig. 1(b). This undercut profile was achieved by dipping the sample in chlorobenzene for 4 minutes prior to development, as suggested in [8].

- 2) *Electron beam lithography*: Next, the samples were spin coated with undiluted spin-on-glass hydrogen silsesquioxane (HSQ) formulated as Fox12 from Dow Corning to a thickness of 70 nm and baked at 90°C for 5 min [9]. HSQ was chosen because of its high resolution (~ 10 nm) and excellent contrast, as well as its good etch resistance and its optical transparency. HSQ is a negative electron beam resist capable of forming nanostructures with low line edge roughness [10]. Fig. 1(c) shows results achieved with HSQ, where we achieved uniform 90 nm wide wires with a 50% fill factor Fig. 1(d) shows isolated NbN lines 50-nm wide with smooth edges. The patterns were written at 30 kV using a Raith 150 electron beam lithography system with a dose of $560 \mu\text{C}/\text{cm}^2$ for large areas and twice that value for narrow isolated lines. Narrow lines required a higher dose because they did not receive a baseline proximity dose from adjacent features. We made use of the conductive NbN beneath the HSQ to prevent charging effects during writes. The samples were developed by immersion in Shipley Microposit MF CD-26 for an hour.
- 3) *Etching*: With HSQ as an etch mask the samples were subtractively patterned with RIE using 95% CF_4 and 5% O_2 . As only 4 nm of NbN was to be removed, the etch did not have to be very anisotropic. Therefore, etching was carried out at 15 mTorr and 100 V DC self-bias potential for 1 min.

C. Description of PMMA-Based Process

In another demonstration, we used samples that had been prepared earlier with a $20 \mu\text{m}$ by $20 \mu\text{m}$ square of 10 nm-thick NbN film connected to gold contact pads. We then patterned the $20 \mu\text{m}$ by $20 \mu\text{m}$ square into the form of a nanowire detector. Although descriptions of similar processes exist [1], [3], we briefly report the details of our process again here for two reasons: (1) it is interesting to note the robustness, reliability, and ease of use of the process; and (2) we used different etching methods than have been reported previously.

We used 950 k molecular weight PMMA spun to 80 nm thick as a positive tone electron beam resist. Narrow lines were written to define the gaps (75 nm) between adjacent lengths of the detector wire. Electron-beam writes were done at 50 kV on an IBM VS26 electron beam lithography tool at a dose of $2400 \mu\text{C}/\text{cm}^2$ and developed in a 3:1 isopropanol (IPA): methyl-isobutyl ketone (MIBK) solution for 2 minutes. To transfer the pattern into the NbN film, we used PMMA as an etching mask and etched the NbN film at 8 mTorr in CF_4 with a 375 V DC self-bias potential. Using this process we fabricated a device over a $15 \mu\text{m} \times 15 \mu\text{m}$ square area with a fill factor of 75%, 225-nm-wide meander lines and 75-nm-wide gaps.

D. Process Damage

In the process of developing the techniques described above, we encountered two unexpected process-damage mechanisms:

- 1) *Plasma damage*: We observed that the very large voltages induced across the device during plasma etching could lead to breakdown across the narrow gaps. This problem can be solved by shorting out the device contacts with a low-impedance short that can be removed after etching.
- 2) *Thermal damage*: We observed thermal damage to the device due to baking. We did a series of control experiments with unpatterned films in which samples were exposed to an array of chemicals and processes to identify those steps that would have an effect on the sample's superconductive properties. The effects that were tested include: O₂ plasma exposure; HF exposure; thermal exposure (baking on a hotplate in ambient atmosphere). We discovered that only baking at 350°C for 5 min destroyed the superconductivity of the samples. Baking at 220°C for 5 min had no effect, and chemical and plasma exposures had no effect.

III. PROXIMITY-EFFECT CORRECTION (PEC)

A. Description of Model

In the fabrication of the detectors, it is important that the nanowires have uniform widths. This constraint is to ensure a uniform current density at all points along the wire. If there were a constriction along the wire, this constriction will act as the “weakest link” in the detector by limiting the maximum current I_c that can flow through the wire. The result is lower detection efficiency; effectively, only the material in the small region around the constriction would be correctly biased to detect single photons.

In electron beam lithography, as electrons penetrate into the resist and substrate they experience forward and backward scattering, thus causing the actual region that gets electron exposure to be much broader than the size of beam tip (~ 2 nm). This is known as the proximity effect. An example of this effect would be that narrow wires written as dense lines (or written close to other large features) are wider than when they are isolated.

In our fabrication process, we applied an optimization method to compensate for proximity effects in the HSQ process. We did not use PEC in the PMMA process. A double-gaussian approximation [8] was used to model the dose received at a point due to forward and backward scattering. The point spread function $\text{psf}(r)$ in this model is:

$$\text{psf}(r) = \frac{1}{\pi(1+\eta)} \left[\frac{1}{\alpha^2} \exp\left(-\left(\frac{r}{\alpha}\right)^2\right) + \frac{\eta}{\beta^2} \exp\left(-\left(\frac{r}{\beta}\right)^2\right) \right].$$

The variables are defined as follows: r is the radial distance from the point of incidence; α is the standard deviation of forward scattered electron distribution; β is the standard deviation of backscattered electron distribution; η is the ratio of backward to forward scattered electron distribution.

For writes at 30 kV, and for sapphire substrates, we used the following parameter values as recommended by the Raith 150 documentation: $\alpha = 0.01 \mu\text{m}$; $\beta = 2.436 \mu\text{m}$; $\eta = 0.5$.

Optimization was performed manually by adjusting relative doses of the large rectangles to the meander lines and by adding dummy features. The cost functions used to optimize the pattern were: (1) the sampled wire width across the meander; and (2) the difference between the highest dose and lowest dose received on the meander lines.

B. Results

The effectiveness of the PEC technique we employed was verified both experimentally and theoretically.

Fig. 2(a) shows the simulation of the meander pattern that was not proximity-effect corrected. With the chosen color map, it is clear that the lines would receive different doses at different parts of the meander. This would cause wires to be wider at the center and narrower at the top and bottom. On the other hand, a proximity-effect corrected pattern (Fig. 2(b)) shows a uniform dose at the meander lines, where it matters most. Dummy features were added to the top and bottom of the meander to achieve this.

We performed electron beam writes for patterns with and without PEC on the same wafer to avoid process variations between runs. Fig. 2(c) shows a portion of a meander pattern written with PEC. We observe very little line edge roughness and highly uniform linewidths. Measurements of linewidths were made at various locations across the meander to confirm the uniformity of lines. The largest variation between any two measurements was ~ 5 nm. On the other hand, the pattern that was written without PEC had a higher variation in linewidths: the largest variation between any two measurements was ~ 15 nm. Fig. 2(d) shows a plot of the linewidth variation for both cases. A larger scatter in measured linewidth was obtained for the uncorrected pattern as expected.

IV. TESTING

A. Testing Methods

We performed initial tests to measure the sheet-resistance (at room temperature) R_s and superconducting transition temperature T_c of the 4 nm thick NbN film on R-plane sapphire substrate. R_s was evaluated by using van der Pauw test structures and Kelvin resistors as shown in Fig. 3(a) and (b) respectively.

Our test equipment consisted of an Agilent 4156C Precision Semiconductor Parameter Analyzer and a cryogenic probe station from Desert Cryogenics. Contact to the sample gold pads was made using single and four-point DC probe tips. Thermal conduction between the samples and the stage was achieved by using a thin layer of indium as a bonding agent.

Throughout the testing procedure, extreme caution was taken in order to prevent damage to the devices from electro-static discharge (ESD). Especially important was ensuring that all electrical contacts were grounded prior to touching the devices. We observed unambiguous examples of devices that were damaged due to poor testing protocol and ESD hygiene.

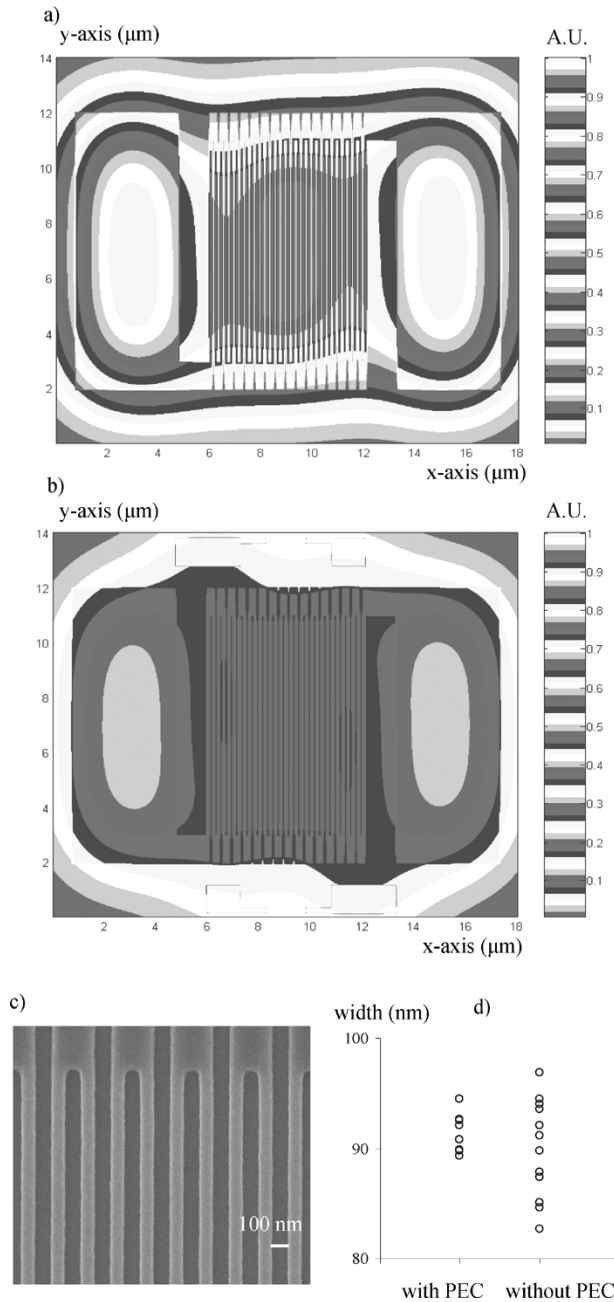


Fig. 2. (a) Simulated dose distribution for an uncompensated meander pattern. The shading was chosen to accentuate any differences in dose of adjacent areas. Due to proximity effect, the wires at the left and right sides of the meander are wider than at the top and bottom. (b) After optimization by adding dummy patterns on the top and bottom of meander and reducing the dose of the large rectangles, wires of more uniform linewidth were obtained. The wires shown here have a dose variation of less than 2% of the total dose. (c) SEM of a portion of the meander pattern written with PEC showing uniform 90 nm wide lines with smooth line edges formed in HSQ. (d) Plot of measured widths at various locations across the meander for proximity effect corrected and uncorrected exposures. With proximity-effect correction a narrower distribution of linewidths was obtained than without proximity-effect correction.

B. Testing Results

Unpatterned and patterned samples were measured to assess the electrical characteristics of the NbN starting material, and the etched nanowires, respectively. Tests of unpatterned samples evaluated the effectiveness of HSQ and PMMA as an

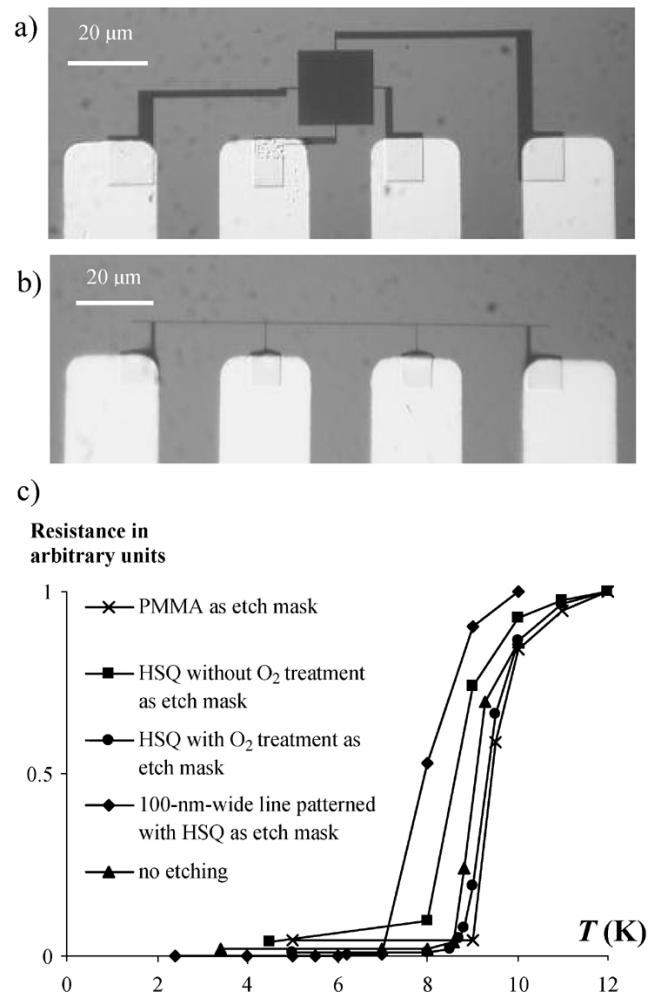


Fig. 3. (a) Optical micrograph of van der Pauw test structure used for sheet resistance measurement. Pattern consists of four gold pads connected to a 20 μm by 20 μm square sheet through narrow wires (400 nm at narrowest points). (b) Optical micrograph of a 200-nm-wide Kelvin-resistor test structure used to evaluate superconductivity of nanowires. (c) Normalized resistance vs. temperature plots showing the effectiveness of HSQ as etch mask in comparison to PMMA. By using HSQ as an etch mask, superconducting wires as narrow as 50 nm could be patterned, but with a T_c reduced by ~ 1 K.

etch mask to ensure that there was no plasma damage to the underlying NbN film. The cage-structured molecules in HSQ experience cross-linking to form extended network structures when exposed to high-energy electrons during electron-beam lithography. During development in Shipley Microposit MF CD-26, the unexposed regions of HSQ dissolve, while the insoluble cross-linked regions remain on the sample surface. This cross-linked HSQ is used as an etch mask in the etching process. To induce cross-linking in the HSQ structure without having to expose the entire sample with electron beam, a HSQ-coated sample was O₂ plasma treated in an asher for 10 min at 100 W power. We assume here that the plasma treatment has the same effect on HSQ as exposure to high-energy electrons does. Fig. 3(c) shows initial test results that both O₂-plasma-treated (i.e. crosslinked) HSQ and PMMA were effective in protecting NbN and were therefore effective etch masks for our process. However, a sample that had been coated with HSQ without O₂ treatment (or electron-beam exposure) appeared to have substantial series resistance.

Measurements of R_s for different devices ranged between 730 Ω/sq and 850 Ω/sq and T_c between 8 K and 9 K for unpatterned films, and $T_c = 7$ K for patterned nanowires.

The test structures appeared to exhibit photosensitive I - V characteristics in DC measurements when exposed to room light. The resistance was observed to increase with increasing light intensity.

V. CONCLUSION

The central result of this work is the development of two processes using proximity-effect-corrected electron-beam lithography to pattern superconductive nanowire single-photon-detector structures. The first method using PMMA allowed us to fabricate meander patterns with a fill factor of 75%. However, we believe that the process we developed using HSQ negative electron resist will help us achieve smoother, narrower wires, [10] and also a high fill factor, leading to an improvement in the detection efficiency. Superconducting NbN wires as narrow as 50 nm have been fabricated that exhibit signs of photosensitivity. Further investigations are needed to fully characterize the devices. We believe this technology can be used to produce high-detection-efficiency, large area GHz-scale-counting rate single photon detectors.

We plan to further develop four aspects of the superconductive single-photon detectors: (1) increase sensitivity by integrating an optical resonant cavity with the device and by reducing the wire width; (2) investigate new superconductive materials as alternatives to NbN; (3) design an on-chip readout circuit; and (4) develop ultra-low-temperature testing methods to improve our understanding of device operation.

An even more useful photodetector could be imagined that would count single photons, identify their wavelength, and determine their polarization at arbitrary bandwidth. Of course, no such detector exists, but the superconductive single-photon detector probably comes closest; it can detect single photons with a reset time of only ~ 70 ps, and theoretically should be able to be used to determine the photon's energy [11] and perhaps even polarization. As this detector is developed, it is likely to open up applications beyond those envisioned to date.

ACKNOWLEDGMENT

Opinions, interpretations, recommendations and conclusions are those of the authors and are not necessarily endorsed by the United States Government.

The authors would like to thank Dr. M. Abraham for extensive technical assistance with the testing, Prof. R. Ram for use of his equipment, Prof. H. I. Smith for use of his equipment and facilities, Mr. M. Mondol for technical assistance with electron-beam lithography, Mr. J. Daley, Mr. J. Carter, Mr. T. Barwicz, Mr. M. Qi, Mr. F. Zhang and Dr. R. Menon for technical assistance and helpful discussions regarding fabrication. They would also like to thank Prof. T. Orlando, Dr. J. Habib, and Dr. R. Hadfield, for helpful discussions.

REFERENCES

- [1] G. Gol'tsman, O. Okunev, G. Chulkova, A. Lipatov, A. Dzardanov, K. Smirnov, A. Semenov, B. Voronov, C. Williams, and R. Sobolewski, "Fabrication and properties of an ultrafast NbN hot-electron single-photon detector," *IEEE Trans. Appl. Supercond.*, vol. 11, pp. 574–577, 2001.
- [2] G. N. Gol'tsman, O. Okunev, G. Chulkova, A. Lipatov, A. Semenov, K. Smirnov, B. Voronov, A. Dzardanov, C. Williams, and R. Sobolewski, "Picosecond superconducting single-photon optical detector," *Appl. Phys. Lett.*, vol. 79, pp. 705–707, 2001.
- [3] G. N. Gol'tsman, K. Smirnov, P. Kouminov, B. Voronov, N. Kaurova, V. Drakinsky, J. Zhang, A. Verevkin, and R. Sobolewski, "Fabrication of nanostructured superconducting single-photon detectors," *IEEE Trans. Appl. Supercond.*, vol. 13, pp. 192–195, 2003.
- [4] R. V. Sobolewski, A. Verevkin, G. N. Gol'tsman, A. Lipatov, and K. Wilsher, "Ultrafast superconducting single-photon optical detectors and their applications," *IEEE Trans. Appl. Supercond.*, vol. 13, pp. 1151–1157, 2003.
- [5] B. Delaet, J. C. Villegier, W. Escoffier, J.-L. Thomassin, P. Feautrier, I. Wang, P. Renaud-Goud, and J.-P. Poizat, "Fabrication and characterization of ultra-thin NbN hot electron bolometer for near infrared single photon detection," *Nuclear Instrum. Methods Phys. Res. A*, vol. 520, pp. 541–543, 2004.
- [6] S. Cherednichenko, P. Yagoubov, K. Il'in, G. N. Gol'tsman, and E. Gershenzon, "Large bandwidth of NbN phononcooled hot-electron bolometer mixers on sapphire substrates," in *Proc. 8th Int. Symp. Space Terahertz Technol.*, Cambridge, MA, 1997.
- [7] A. D. Semenov, G. N. Gol'tsman, and A. A. Korneev, "Quantum detection by current carrying superconducting film," *Physica C*, vol. 351, pp. 349–356, 2001.
- [8] M. Hatzakis, B. J. Canavella, and J. M. Shaw, "Single-step optical lift-off process," *IBM J. Res. Develop.*, vol. 24, pp. 452–460, 1980.
- [9] W. Henschel, Y. M. Georgiev, and H. Kurz, "Study of a high contrast process for hydrogen silsesquioxane as a negative tone electron beam resist," *J. Vacuum Sci. Technol. A (Vacuum Surfaces, Films)*, vol. 21, pp. 2018–2025, 2003.
- [10] H. Namatsu, T. Yamaguchi, M. Nagase, K. Yamasaki, and K. Kurihara, "Nano-patterning of a hydrogen silsesquioxane resist with reduced linewidth fluctuations," *Microelectron. Eng.*, vol. 41–42, pp. 331–334, 1998.
- [11] A. Verevkin, J. Zhang, R. Sobolewski, A. Lipatov, O. Okunev, G. Chulkova, A. Korneev, K. Smirnov, G. N. Gol'tsman, and A. Semenov, "Detection efficiency of large-active-area NbN single-photon superconducting detectors in the ultraviolet to near-infrared range," *Appl. Phys. Lett.*, vol. 80, pp. 4687–4689, 2002.